
Micro-structure Selection in Solid-solid Transitions: A Review

Jayee Sinha*

Abstract

Solid – solid phase transitions are invariably associated with group of particles whose deformations cannot be expressed as an affine strain about a reference configuration. Using molecular dynamics simulations, we study the nucleation dynamics and microstructure selection in a model two-dimensional solid undergoing a square to rhombic transformation. The microstructure selection depends on the depth and rate of quenching. The nucleation process is initiated by the appearance of distinct dynamical heterogeneities. It is observed that the dynamics of the non - affine zones (NAZs) determine the subsequent growth of the microstructure within the parent solid. The nature of particle trajectories in the active regions show an abrupt transition from ballistic to diffusive behaviour which remarkably coincides with the sharp and discontinuous transition from a twinned martensite to a ferrite microstructure. The active particles exhibit intermittent jamming and un-jamming. At low temperatures, single particle diffusion is suppressed and the transformation proceeds through string – like correlated excitations, giving rise to the twinned martensite nuclei. These excitations flow along ridges in the potential energy topography set up by the inactive particles. At higher temperatures, the trajectories of the particles show the transition from ballistic to diffusive nature giving rise to the ferrite nuclei.

Copyright © 2018 International Journals of Multidisciplinary Research Academy. All rights reserved.

Keywords:

Microstructure;
Nucleation;
Phase transitions;
Martensite;
Ferrite.

Author correspondence:

Jayee Sinha,
Department of Electronic Science
University of Calcutta, 92 Acharya Prafulla Chandra Road, Kolkata – 700009, West Bengal , India
Email: jselc@caluniv.ac.in

1. Introduction

The study of microstructure selection in solid state transitions is particularly challenging when it relates multiscale physics, from atomic trajectories to mesoscale ordering. The dynamics following a quench schedule in solid-solid phase transitions rarely takes the solid to its equilibrium state. The quench across a solid-solid transformation generally results in a product solid with different microstructures having a specific ordering of atoms [1, 2] The nature of microstructure depends not only on symmetry relations between parent and product but on quench protocols such as depth and rate of quenching. Borrowing terminology from the microstructure of steel [3], commonly characterized microstructures are ferrite and twinned martensite which differ greatly in their properties. At high temperatures, nucleation and growth gives rise to the isotropic, polycrystalline ferrite microstructure associated with a disorderly movement of atoms. The elasticity of the solid has no significant role in determining the ferrite microstructure. In contrast, at low temperatures, nucleation and growth is largely influenced by the elasticity of the solid and hence results in a twinned,

*Department of Electronic Science, University of Calcutta, 92 Acharya Prafulla Chandra Road, Kolkata – 700009, West Bengal, India

anisotropic martensite microstructure. The twinned structure arises due to the coordinated motion which often results in alternating variants of the product sharing a common crystallographic mirror plane (twins).

These two microstructures are the two possibilities and they are not mutually exclusive. The selection for growth of microstructure with time depends on the dynamical phase diagram. Here, in this paper we review the dynamical phase diagram along with the quench protocols which provides a deeper understanding of solid state nucleation and growth mechanism.

We consider a two dimensional model solid to study the phase transformations associated with the quench protocols using molecular dynamics simulations. It is observed that internal stresses generated during the transformation create local non-affine zones (NAZ) beyond a threshold stress [4]. The dynamics of these NAZs determines the selection of the microstructure. The paper is organized as follows. In the next section, we describe the model solid and the molecular dynamics simulations for the square to rhombic transition. Section 3 contains the results and its analysis, identification of NAZs and their evolution during the solid state transformation.

It is seen that accommodation of interfacial mismatch occurs by the appearance of dynamical heterogeneities in the transforming solid. The thermodynamics of space-time trajectories of active particles is also analysed and such particles exhibit intermittent jamming and un-jamming. Topography of the inactive and active particles along with the active particle trajectories also depicts the formation of the isotropic and anisotropic microstructures at different temperatures. The paper ends with a summary and conclusion in section 4.

2. Research Method (12pt)

The two-dimensional model which shows transitions between square and rhombic (a special case of the more general oblique lattice) lattices comprises of particles confined within a box. They interact via an effective potential [5] which is the sum of an anisotropic two-body potential and a three-body potential, the representations for which is given as follows:

$$V=1/2 \sum_{i \neq j} V_2 (r_{ij}) + 1/6 \sum_{i \neq j \neq k} V_3 (r_i, r_j, r_k) \quad (1)$$

where r_i is the position vector of particle i and $r_{ij} \equiv |r_{ij}| \equiv |r_j - r_i|$. The anisotropic two-body potential is purely repulsive and short ranged with :

$$V_2(r_{ij}) = v_2 \left(\frac{\sigma_0}{r_{ij}}\right)^{12} \{1 + \alpha \cos^2 2\theta_{ij}\} \quad (2)$$

where σ_0 and v_2 set the units of length and energy, α is an ‘anisotropic lock-in’ parameter and θ_{ij} is the angle between r_{ij} and an arbitrary external axis. The short-ranged three-body interaction is given as

$$V_3(r_i, r_j, r_k) = v_3 [f_{ij} f_{jk} \sin^2 4\theta_{ijk} + \text{permutations}] \quad (3)$$

where the function $f_{ij} \equiv f(r_{ij}) = (r_{ij} - r_0)^2$ for $r_{ij} < r_0 = 1.8\sigma_0$ and 0 otherwise. The angle θ_{ijk} is the angle between the vectors r_{ij} and r_{jk} . The two-body and three-body interactions favour rhombic and square ground states, respectively. Inclusion of the two-body anisotropic lock-

in parameter α helps to vary the jump in the order parameter from strongly first order ($\alpha = 0$) to a continuous transition for $v_3 = 0, \alpha \sim 1.5$.

The rhombic lattice is a special case of the general oblique lattice—one of the five possible two-dimensional Bravais lattices. In general, we need two order parameters to describe the transition between square and oblique lattices. They are the affine shear strain $e_3 = \epsilon_{xy} = \epsilon_{yx}$ and the deviatoric strain $e_2 = \epsilon_{xx} - \epsilon_{yy}$ [6]. Considering the square lattice as the reference, the microscopic model produces a rhombic lattice for which e_2 identically vanishes and the four equivalent variants merge in pairs to give *two* symmetry-related rhombic products. The value of e_2 is zero and therefore it is sufficient to use e_3 as the sole order parameter for the transition.

The unit of time in our simulations is $\sigma_0 \sqrt{m/v_2}$, where m is the particle mass. Using typical values, this translates to a simulation time unit of 1 ps. Individual particle trajectories obtained during the simulation, allows us to project time dependent atomic positions leading to different microstructures.

Both the two-body and three-body potentials are purely repulsive and therefore the system needs to be confined either in a box of fixed volume or by an external compression. The molecular dynamics simulations are performed in the constant number, volume (and shape) and temperature (NVT) ensemble with periodic boundary conditions using a Nose–Hoover thermostat [7]. The equations of motion for up to $N = 12099$ particles are integrated using a Verlet scheme with a time step $t = 10^{-3}$. The relaxation time of the Nose–Hoover thermostat determines how fast the system relaxes to the ambient temperature. However, the results are robust to its changes within reasonable limits.

3. Results and Analysis

3.1. Results from quench protocols

Figure 1(a) is the phase diagram obtained in the $T-v_3$ plane (with $\alpha = 0$). The solid line is the phase boundary between square and rhombic crystals. The dashed line marks the temperature above which anisotropic, twinned nuclei become rare and is identified as the martensite start (or M_s) temperature for the model. Typical product nuclei formed following quenches at high and low temperatures are shown in figure. 1(b). The top one is the isotropic ferrite formed at $T = 0.8$ for a quench of ($v_3 = 10 \rightarrow 5.5$) and the bottom is the anisotropic, twinned martensite formed at $T = 0.1$ for a quench of ($v_3 = 5 \rightarrow 1.65$). Both are obtained starting with an equilibrated square parent crystal composed of 12099 particles which consists of a seed (vacancy or a smaller sized particle) to initiate the nucleation process. The process of seeding is a matter of convenience at higher temperatures but it is necessary at lower temperatures since in this case the transformation proceeds through heterogeneous nucleation. The ferrite microstructure formed due to homogeneous nucleation is polycrystalline in nature consisting of grains of the rhombic crystal. On the other hand, the martensite microstructure has a twinning interface where the shear strain changes its sign.

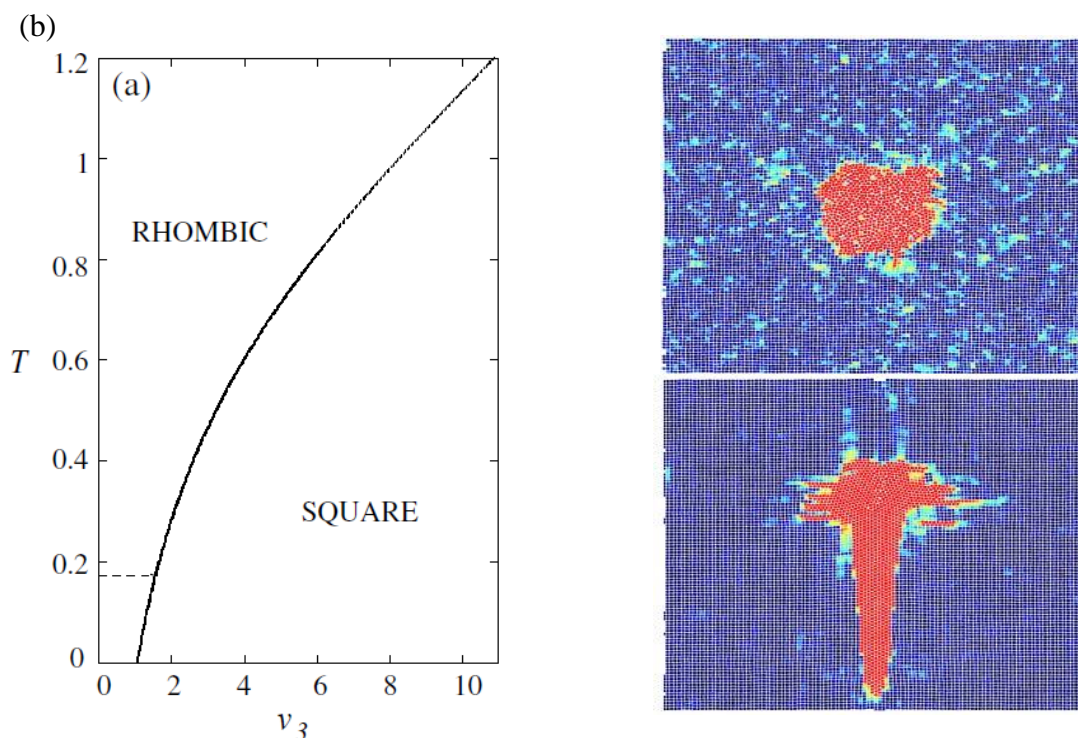


Figure 1. (a) Phase diagram in the $T-v_3$ plane (with $\alpha = 0$), (b) The top one is the isotropic ferrite at $T = 0.8$ for a quench of ($v_3 = 10 \rightarrow 5.5$) and the bottom is the anisotropic, twinned martensite at $T = 0.1$ for a quench of ($v_3 = 5 \rightarrow 1.65$). Both are obtained starting with an equilibrated square parent crystal composed of 12099 particles.

3.2. Non-affine zones (NAZs), active and inactive particle trajectories

In both the phases obtained from different quench schedules, the nucleation of the product is accompanied by the formation of non-affine zones (NAZs) characterized by the non-affine parameter whose magnitude is larger than a given threshold [4]. To calculate and quantify the non-affineness leading to the NAZs the coarse-grained local strain field is obtained using the procedure in [8]. The immediate neighborhood, (defined using a cutoff distance equal to the range of the potential) centered around \mathbf{r} , of any tagged particle 0 in the initial reference lattice (at time $t = 0$) is compared with that of the same particle in the transformed lattice. The ‘best-fit’ local affine strain ϵ_{ij} is obtained which maps as nearly as possible all the particles n in Ω from the reference to the transformed lattice using an affine connection. This is done by minimizing the (positive) scalar quantity:

$$(4) \quad D_{\Omega}^2(r, t) = \sum_{n \in \Omega} \sum_i \left\{ r_n^i(t) - r_0^i(t) - \sum_j (\delta_{ij} + \epsilon_{ij}) \times (r_n^j(0) - r_0^j(0)) \right\}^2$$

with respect to choices of affine ϵ_{ij} . Here, again, the indices i and $j = x, y$, and $r_n^i(t)$ and $r_n^i(0)$ are the i th component of the position vector of the n th particle in the transformed and reference lattice, respectively. Any *residual* value of $D_{\Omega}^2(r, t)$ is a measure of non-affineness. It is clear from figure 2(b) that the NAZ covers the entire growing nucleus in the ferrite phase while it is restricted to and advected by the growing front in the martensite phase (figure 2(a)). The nucleation and growth of the product in the mesoscale is initiated by the movement of a small fraction of particles having the top 10% of the kinetic energy, which are termed as the active particles and they are surrounded by regions of inactive

particles. These active particles form isolated clusters and they are termed as dynamical heterogeneities [9]. The NAZs typically overlap with these dynamical heterogeneities.

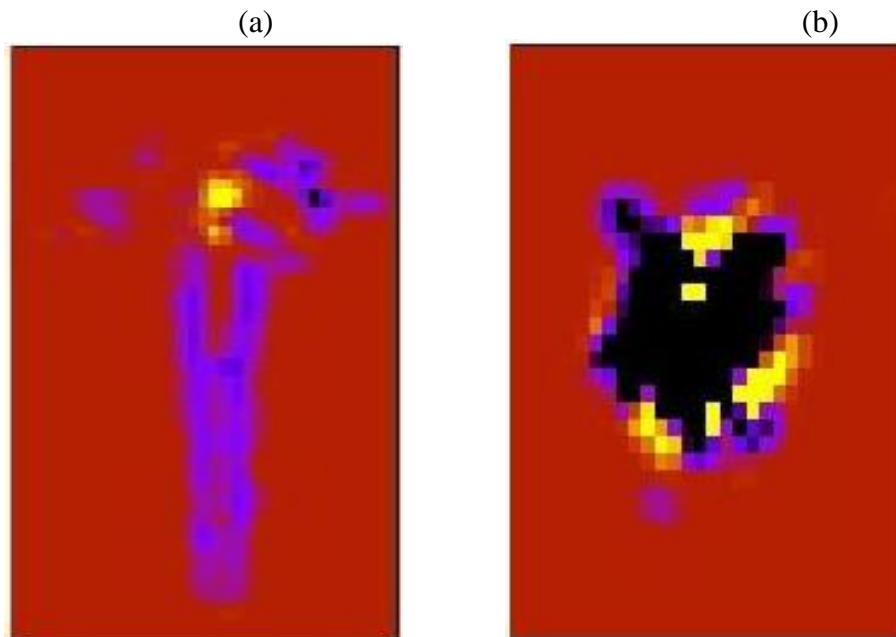


Figure 3. Non-affine deformation with colors ranging from -1 to 1 . (a) In martensite, NAZs surround the growing nucleus and are created at and advected by the front. It is absent at the centre of the nucleus. (b) In ferrite, non-affine regions are present throughout the interior of the nucleus, signifying extensive plastic deformation during growth.

The dynamics of active particles which accompany the growing nucleus after a quench can be observed by analyzing the spacetime trajectories within and in the vicinity of the dynamical heterogeneities in the form of kymographs, shown in figure 3. In the martensite phase, the active particles move ballistically and in a coordinated manner; the tagged particle velocity correlation is significant both along a single trajectory and across neighboring trajectories at equal time. Figure 3(i) plots the dynamics of a contiguous set of particles along a line. There is a large surge of activity at $t \approx 2$ where several particles become active denoted by red lines. The correlated jamming and unjamming exhibited by these particles is seen in the termination and emergence of the red line segments. Panels (ii) and (iii) show similar behavior. The mean number of active particles grows with time, with the older active particles seeding newer ones. The highly coordinated movement, characteristic of a martensite is apparent in these kymographs. The arrest of all active particles within a dynamical heterogeneity happens roughly simultaneously. On the other hand, in figure 3 ,panels (iv)–(vi) similar plots for the ferrite phase at $T = 0.7$ have larger number of active particles. Their trajectories intersect many times and tagged particle trajectories are diffusive over timescales. The active particles in the martensite are concentrated near the edge of the single growing nucleus, while in the ferrite they are distributed. The particles in both phases continuously transform between active and inactive states.

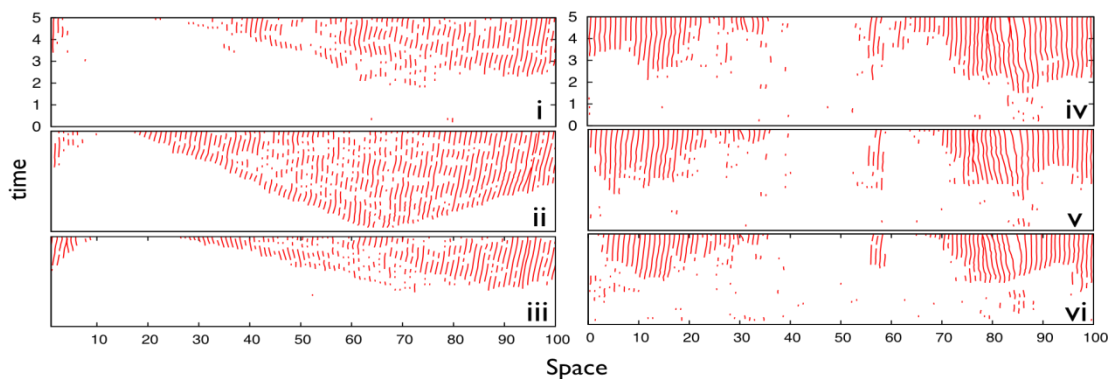


Figure 3. Spacetime kymographs denoting particle trajectories y versus t for fixed x .

Figures (i)–(iii) correspond to the martensite phase at $T = 0.1$ at $x = 50, 55$ and 60 . Figures (iv)–(vi) are kymographs for the ferrite phase, at $T = 0.6$, along the lines $x = 55, 66$ and 97 .

3.3. Potential energy topography

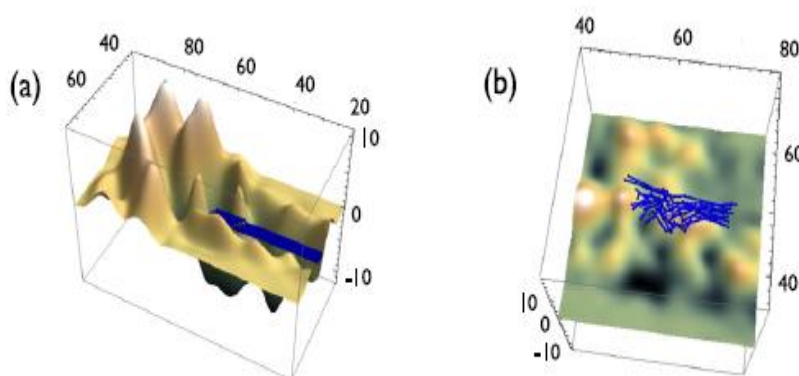


Figure 4. Topography of the potential energy due to the inactive particles. (a) Deep ridges direct the flow of the active particles in a string-like motion in the twinned martensite phase and (b) in the ferrite phase, the active particle trajectories diffusively span out isotropically.

The topography of the potential energy is set up by the inactive particles. From the particle coordinates, local values for the coarse-grained strain components are calculated and used in the expression of elastic energy density [5,9] to obtain an adequate representation of the local potential energy topography. Figure 4(a), corresponds to the martensite phase, which consists of high ridges in the local potential energy surface with the active particles moving along a narrow channel where their trajectories do not intersect. The width of the string is of the order of the lateral scale of the dynamical heterogeneities. The inactive, jammed, particles on the ridge surrounding the channel represent regions of large stresses resulting in large values of the free energy. In the ferrite phase, the landscape exhibits several shallow ridges which directs the particles here and there. The trajectories span out isotropically, leading to diffusive collective excitations. Thus the difference in the spacetime trajectories arises from the kinetic constraints on active particles created by the slowly evolving energy landscape due to inactive particles.

4. Conclusion

In this paper, the dynamics of microstructure selection in solid-solid transitions has been explored using molecular dynamics simulations on a model two-dimensional solid. Variation in the quench protocol following the phase diagram supports the nucleation and growth of microstructures at different temperatures. At low temperatures the anisotropic, twinned martensite is formed while at higher temperatures with deeper quenching, isotropic polycrystalline ferrite is obtained. The transformation is accompanied by transient, localized regions of plasticity called NAZs. The dynamics of these NAZs play a vital role in microstructure selection. The dynamical heterogeneities are defined by clusters of active particles which move in a static background of inactive particles which provides the topography of the confining potential energy. Thus, when the local potential energy has deep ridges, the particle excitations are string-like, while on the other hand, when the potential energy is a shallow delta, the excitations are diffusive. This change in the nature of active particle trajectories happens abruptly when a parameter, such as temperature, is varied. Therefore the phase transition is characterized in terms of a spacetime thermodynamics of trajectories which drives the selection of microstructure. The study provides a link between microscopic particle trajectories and mesoscopic microstructure of the product solid.

Acknowledgements

The author gratefully acknowledges the support and guidance received from S. Sengupta and M. Rao. Also computation support from Satyendra Nath Bose National Centre for Basic Sciences is highly acknowledged.

References

- [1] R. W. Cahn and P. Haasen, *Physical Metallurgy*, North-Holland, Amsterdam, 1996.
- [2] R. Phillips Crystals, *Defects and Microstructures: Modeling Across Scales*, Cambridge University Press, Cambridge, 2001.
- [3] A. G. Kachaturyan, *Theory of Structural Transformations in Solids*, New York, Wiley, 1983.
- [4] J. Bhattacharya, A. Paul, S. Sengupta and M. Rao, "Non-affine deformation in microstructure selection in solids: I. Molecular dynamics" *J. Phys.: Condens. Matter*, vol. 20, pp. 365210, 2008.
- [5] M. Rao and S. Sengupta, "A mesoscopic model of a two-dimensional solid state structural transformation: statics and dynamics", *J. Phys.: Condens. Matter*, vol. 16, pp. 7733, 2004.
- [6] M. Rao and S. Sengupta, "Nucleation of Solids in Solids: Ferrites and Martensites", *Phys. Rev. Lett.*, vol. 91, pp. 045502, 2003.
- [7] D. Frenkel and B. Smit, *Understanding Molecular Simulations* 2nd edn, New York: Academic, 2002.

- [8] M. L. Falk and J. S. Langer, “Dynamics of viscoplastic deformation in amorphous solids”, *Phys. Rev. E*, vol. 57, pp. 7192, 1998.
- [9] S. Sengupta, M. Rao and J. Bhattacharya, “Early-time particle dynamics and non-affine deformations during microstructure selection in solids”, *J. Phys.: Condens. Matter*, vol. 23, pp. 295402, 2011.